Truncation of the N-terminus of cardiac troponin I initiates adaptive remodeling of the myocardial proteosome via phosphorylation of mechano-sensitive signaling pathways

Chad Warren, Monika Halas, Paul Goldspink, Han-Zhong Feng, Anthony Herren, Beata Wolska, Pieter de Tombe, Jian-Ping Jin, R. John Solaro

Truncation of the N-terminus of cardiac troponin I initiates adaptive remodeling of the myocardial proteosome via phosphorylation of mechano-sensitive signaling pathways

Chad M. Warren[1] · Monika Halas[1] · Paul H. Goldspink[1] · Han-Zhong Feng[1,2] · Anthony W. Herren[3] · Beata M. Wolska[1,4] · Pieter P. de Tombe[1,5] · Jian-Ping Jin[1,2] · R. John Solaro[6]

Abstract

The cardiac isoform of troponin I has a unique N-terminal extension (~ 1–30 amino acids), which contributes to the modulation of cardiac contraction and relaxation. Hearts of various species including humans produce a truncated variant of cardiac troponin I (cTnI-ND) deleting the first ~ 30 amino acids as an adaption in pathophysiological conditions. In this study, we investigated the impact of cTnI-ND chronic expression in transgenic mouse hearts compared to wildtype (WT) controls (biological $n = 8$ in each group). We aimed to determine the global phosphorylation effects of cTnI-ND on the cardiac proteome, thereby determining the signaling pathways that have an impact on cardiac function. The samples were digested and isobarically labeled and equally mixed for relative quantification via nanoLC-MS/MS. The peptides were then enriched for phospho-peptides and bioinformatic analysis was done with Ingenuity Pathway Analysis (IPA). We found approximately 77% replacement of the endogenous intact cTnI with cTnI-ND in the transgenic mouse hearts with 1674 phospho-proteins and 2971 non-modified proteins. There were 73 significantly altered phospho-proteins; bioinformatic analysis identified the top canonical pathways as associated with integrin, protein kinase A, RhoA, and actin cytoskeleton signaling. Among the 73 phospho-proteins compared to controls cTnI-ND hearts demonstrated a significant decrease in paxillin and YAP1, which are known to play a role in cell mechano-sensing pathways. Our data indicate that cTnI-ND modifications in the sarcomere are sufficient to initiate changes in the phospho-signaling profile that may underly the chronic-adaptive response associated with cTnI cleavage in response to stressors by modifying mechano-sensitive signaling pathways.

Keywords Cytoskeleton · Heart · Integrin · Mouse · Sarcomeres · Paxillin

Introduction

Cardiac troponin I (cTnI) is specifically expressed in vertebrae adult hearts. Studies from our laboratories have identified a stress-induced [1–3] restrictive proteolysis of cTnI, the inhibitory unit of the cTn complex. The proteolysis produces an NH_2 deletion (cTnI-ND), deleting 27–30 amino acids of the cTnI-specific NH_2-terminal extension. Functionally, this region of cTnI has protein kinase A (PKA) phosphorylation sites critical in the control of cardiac relaxation reserve [4, 5]. Recent studies employing paramagnetic resonance enhancement have proposed that the dephosphorylated NH_2-terminal extension of cTnI interacts with the Ca^{2+} regulatory site II of cardiac troponin C (cTnC) and the region interacting with the cTnI switch peptide [6]. Moreover, they showed that phosphorylation of the NH_2-terminal extension weakens

✉ R. John Solaro
solarorj@uic.edu

1 Department of Physiology & Biophysics, Center for Cardiovascular Research, University of Illinois at Chicago, Chicago, USA

2 Department of Physiology, Wayne State University School of Medicine, Detroit, MI, USA

3 UC Davis Genome Center, Davis, CA, USA

4 Division of Cardiology, Department of Medicine, University of Illinois at Chicago, Chicago, USA

5 Phymedexp, Université de Montpellier, Inserm, CNRS, Montpellier, France

6 Department of Physiology & Biophysics, College of Medicine, Center for Cardiovascular Research, University of Illinois at Chicago, 835 South Wolcott Avenue RM. E-202 (M/C 901), Chicago, IL 60612, USA

these interactions promoting the release of the cTnI switch peptide. These data align with other findings that removal of the NH_2-terminal extension mimics the effects of phosphorylation [7]. A tyrosine kinase phosphorylates cTnI at Tyr 26 resulting in a depression in the Ca^{2+} sensitivity of the myofilaments in skinned fiber preparations. The absence of this site in cTnI-ND may contribute mechanistically to the cardioprotection associated with the presence of cTnI-ND [8].

We consider the restrictive proteolysis of cTnI-ND to be an adaptive response [1–3, 7, 9]. Data in support of this idea demonstrated that expression of cTnI-ND in a transgenic model improves cardiac function in response to pathological (β-adrenergic signaling deficiency) [3] and physiological (aging) stressors [9]. Within the context of these stressors, one mechanism responsible for the improvements in cardiac contractility found in the cTnI-ND mice may involve alterations at the level of the myofilaments. These results also indicate that persistent expression of cTnI-ND induces cardiac remodeling associated with improved function in aging. Despite these phenotypic improvements the mechanisms involved to explain the long-term effects of cTnI-ND expression on signaling networks beyond the sarcomere remain to be elucidated.

To explore the nature of the signaling events beyond the sarcomere, we hypothesized that adaptive remodeling of the heart with long-term expression of cTnI-ND may manifest in signaling pathways regulated by phosphorylation. To test this hypothesis, we employed bottom-up proteomics to quantify phospho-peptides obtained from isobaric-labeled samples from hearts of control mice expressing cTnI-WT and transgenic mice expressing cTnI-ND. Bioinformatic analysis of the 73 differentially phosphorylated proteins identified revealed they were enriched in pathways associated with integrin, protein kinase A, RhoA, and actin cytoskeleton signaling. Our results show that this proteolytic modification of cTnI results in adaptive myofilament biophysical changes that trigger alterations in signaling pathways associated with mechano-sensing in the heart.

Materials and methods

Animals

The animal care and use committee of the University of Illinois at Chicago approved all animal protocols, which also conforms to the "Guide for the Care and Use of Laboratory Animals" published by the United States National Institutes of Health, 8th edition, revised 2011. All animals used in this study were 3–5 months old and from a C57BL/6 strain. The transgenic mice expressing cTnI-ND ($n=8$), an N-terminal 1–28 amino acid deletion, were heterozygotes as previously described [7] and the non-transgenic littermates were used as negative controls cTnI-WT ($n=8$).

Western blot analysis

Western blot analysis was performed as previously described [10] for all experiments. The primary and secondary antibodies used to probe the membranes are listed in Table 1 along with the dilutions. The membranes were incubated with SuperSignal West Femto maximum sensitivity substrate reagent from Thermo Scientific and imaged with Bio-Rad's Chemidoc MP. Immunoblot images were analyzed with Image Lab v. 6.0.1 Bio-Rad and GraphPad Prism 8.

Heart protein sample preparation for tandem mass tag (TMT) labeling

The C57BL/6 mice (cTnI-WT and cTnI-ND) were anesthetized with a mixture of 200 mg/kg ketamine and 20 mg/kg xylazine, per the American Veterinary Medical Association Panel on Euthanasia Guidelines 2013. A cardioectomy was

Table 1 Antibodies used for Western blot analysis

Antibodies	Catalog #	Supplier	Location	Dilution
M-mAb anti-cardiac troponin I	10R-T123K	Fitzgerald Industries International	Acton, MA	1:5000 5% NFDM + TBST
M-mAb anti-actin	10R-7820	Fitzgerald Industries International	Acton, MA	1:2000 5% NFDM + TBST
R-pAb anti-actin	PA1-16889	Thermo Fisher Scientific	Waltham, MA	1:5000 5% NFDM + TBST
R-pAb anti-paxillin	32084	Abcam Inc	Cambridge, MA	1:2500 5% NFDM + TBST
R-pAb anti-phospho-paxillin (y31)	4832	Abcam Inc	Cambridge, MA	1:1000 1% BSA + TBST
R-pAb anti-phospho-cardiac troponin I (S23/24)	4004S	Cell Signaling Technology	Danvers, MA	1:1000 5% NFDM + TBST
Goat anti-Rabbit IgG HRP-linked	7074S	Cell Signaling Technology	Danvers, MA	1:20,000 5% NFDM + TBST
Horse anti-mouse IgG HRP-linked	7076S	Cell Signaling Technology	Danvers, MA	1:20,000 5% NFDM + TBST

M-mAb mouse monoclonal antibody, *R-pAb* rabbit polyclonal antibody, *NFDM* non-fat dry milk, *TBST* tris-buffered saline with 0.1% (v/v) Tween-20

performed and the heart tissue was stored at − 80 °C. The frozen heart tissue (10–15 mg) was homogenized in lysis buffer 1:20 (w/v) (8 M urea, 50 mM TEAB pH 8.5, phosphatase inhibitor set 1 1:100 (v/v) EMD Millipore, 100 nM Calyculin A, and 10 mM TCEP) with an Omni International Bead Ruptor Elite (0.5 mL tube, 1.4 mm ceramic bead) set at power 4 m/s, 15 s, three cycles with 3-min dwell between cycles. The samples were then centrifuged in a 4 °C microfuge at max speed for 3 min to clarify the supernatant fraction was reserved as the sample. The sample concentrations were determined with Pierce's 660 nm protein assay following the manufacturer's recommendations. To make a global standard, 5 µl of all equally diluted samples were mixed and used as a control for comparing the cTnI-WT vs. cTnI-ND. The samples and 4 replicate global standards (125 µg) were alkylated with 30 mM Iodoacetamide for 30 min at room temperature protected from light and then quenched with 20 mM DTT incubated for 15 min at room temperature.

To digest the samples first Lys-C (WAKO) was added at 1:100 enzyme:substrate ratio and incubated for 5 h at 37 °C in an Eppendorf ThermoMixer C. After the 5-h incubation the samples were diluted with 50 mM TEAB pH 8.5 until the urea concentration was at 1 M and then trypsin (Promega gold) was added at a 1:25 enzyme:substrate ratio and left to digest overnight (16 h) at 37 °C. The digested samples were then equally labeled with 10-plex TMT (ThermoScientific) following the manufacturer's recommendations. The 126 and 130N channels of the 10-plex TMT were used for the global standards for two independent experiments where a biological n in each experimental group was 4 for a combined total of 8 in the study. The TMT channels were swapped between groups and experiments to help minimize any labeling bias except for the global standards which were 126 and 130N throughout the study. After quenching the labeling reaction, all samples were mixed equally and speed vac down to dryness.

Phospho-enrichment and high-pH reversed-phase fractionation

The dried TMT-labeled peptides were then resuspended in 300 µL of 2% (v/v) TFA to clean up the peptides in a peptide desalting spin column (Thermo Scientific Cat# 89852) following the manufacturer's recommendations with minor modifications. Briefly, after binding the sample to the column the flow through and the first 100 µL wash was saved. The rest of the washes was as suggested by the manufacturer. The elution was done three times instead of twice. The saved flow through and first wash was then loaded onto a Pierce graphite spin column (cat# 88302) to further capture and desalt peptides in series. The graphite protocol was followed as suggested by the manufacturer except for minor modifications. The elution was done with 100 µL of suggested elution buffer twice and then the combined fractions were reapplied to the column two more times. The elutions from the serial peptide clean-ups were combined and speed vac to dryness. The dried peptide was resuspended in 100 µL of 25% (v/v) acetonitrile and 0.1%TFA (v/v), and a colorimetric peptide assay (Thermo Scientific #23275) was performed as suggested to determine peptide concentration and separate into two aliquots containing 5% and 95% of the total peptides. The 5% aliquot was saved for non-enriched peptides also known as the "total" and speed vac to dryness. The 95% aliquot was saved for phospho-peptide enrichment by Sequential enrichment of Metal Oxide Affinity Chromatography (High-Select™ SMOAC) (Thermo Scientific # A32993 and A32992) following the manufacturer's recommendations. The phospho-peptide enrichment was first done with TiO_2 and then Fe-NTA serially performed as suggested by the manufacturer. The eluted phospho-peptides were combined and speed vac to dryness and stored at − 80 °C.

To fractionate both the non-enriched and phospho-peptide-enriched samples, we used a Pierce High-pH Reversed-Phase peptide fractionation kit (Cat# 84868) with modifications. The column was conditioned, and the peptides were resuspended as suggested by the manufacturer. A 300 µL sample was loaded into the column twice and then washed twice with 300 µL of 0.1% TFA and once with 300 µL of water. We used a revised elution table with 12 fractions and each receiving microfuge tube had 30 µL of 10% (v/v) formic acid in it before starting the elution to quickly acidify the peptides after elution. The revised elution table kept the proportion of acetonitrile and 0.1% (v/v) triethylamine the same as in the suggested protocol, but we changed the acetonitrile percentages and added 4 fractions. The acetonitrile percentages for the fractions were 0, 2.5, 5, 7.5, 10, 12.5, 15, 17.5, 20, 22.5, 25, and 80. The peptide concentrations of the fractions were determined with a colorimetric peptide assay kit (Thermo Scientific # 23275) and the phospho-peptide fractions were concatenated into five fractions from 12. The non-enriched "total" had 10 fractions where the first fraction was discarded, and the 11th and 12th were combined. The fractions were then speed vac down to dryness and stored at − 80 °C until run on a Thermo Scientific Fusion Lumos Orbitrap Mass Spectrometer.

Synchronous precursor selection (SPS) MS^3 Mass Spectrometric data acquisition

Digested TMT-labeled peptide fractions were reconstituted in 2% acetonitrile/0.1% TFA and analyzed on a Thermo Scientific Fusion Lumos Orbitrap Mass Spectrometer in conjunction with an UltiMate 3000 RSLCnano UHPLC and EASY-Spray source operating in positive ionization mode as previously described with minor modifications

[11]. Either half of the reconstituted yield (for phospho-enriched) or 1 µg (for total) of peptides were loaded on a Thermo Scientific Acclaim PepMap 100 C18 reversed-phase pre-column (DX164199, 100 µm × 20 mm, 100 Å, 5 µm) before being separated using an EASY-Spray C18 reversed-phase analytical column (ES802, 75 µm × 250 mm, 100 Å, 2 µm). Peptides were eluted with an increasing percentage of acetonitrile (0–50%) throughout a 180-min gradient with a flow rate of 200 nl/min at 40 °C. An MS survey scan was obtained for the m/z range 350–1600 and acquired with an orbitrap resolution of 120,000 and a target of 5×10^5 ions or a maximum injection time of 50 ms (msec). Data-dependent MS/MS spectra were acquired in the linear ion trap using CID (Collision-Induced Dissociation) for fragmentation at 35% energy with an activation Q of 0.25. MS/MS spectra were acquired in turbo mode with a target of 1×10^4 ions or a maximum injection time of 50 ms. An isolation mass window of 0.7 m/z was used for precursor ion selection, charge states 2–7 were accepted, and a 60-s duration was used for dynamic exclusion. Using synchronous precursor selection, up to 10 precursors were then selected for higher-order MS3 detection in the orbitrap following further fragmentation using HCD (Higher-Energy Collision Dissociation) at 65% energy. A mass range of 100–500 m/z was scanned with a resolution of 50,000 and acquired with a target of 1×10^5 ions or a maximum injection time of 105 ms. A precursor selection range of 400–1200 m/z was used with an isolation window of 2 m/z. The cycle time was fixed at 3 s.

Mass spectrometric data analysis

Raw data-dependent acquisition files of fractions were combined and searched in Proteome Discoverer (version 2.3.0.523) using default processing and consensus workflow settings for tribrid TMT 10-plex reporter ion SPS MS3-based quantitation with changes as noted below. Briefly, the PMI-Byonic node (version 3.4) was used for a target-decoy search strategy against a mouse sequence database (downloaded Feb 22, 2019, from Uniprot.org with 17,008 entries), and identifications were made at a false discovery rate (reversed decoy database) of 1% at the protein level. The ptmRS node was used to report phosphosite localization with diagnostic ions. Searches were configured for a precursor ion mass tolerance of 20 ppm, a fragment ion mass tolerance of 0.2 Da, trypsin allowing for 2 missed cleavages, carbamidomethyl of Cys, TMT6-plex addition of Lys, and TMT6-plex addition of the peptide N terminus as static modifications. Dynamic modifications included phosphorylation of Ser, Thr, and Tyr; oxidation of Met; and deamidation of Asn and Gln.

For phospho analysis, TMT reporter-based quantitation was performed using a co-isolation threshold of 65, an average S/N threshold of 1, and an SPS mass match tolerance of 20%. Isotopic distribution corrections were applied to all channels based on Lot #TJ268160. Normalization was done against the sum of total peptide abundance using all peptides with scaling against the average of all four global-pooled standards. In general normalization was applied for each channel across all files, equalizing the total abundance between different runs. The normalization factor was determined from the sum of the sample and the maximum sum in all files (cTnI-WT, cTnI-ND, and global-pooled standard). After aggregating all the normalized abundance values per sample, the four global-pooled standard samples were scaled so that the average of all four global-pooled standards were 100 and then all other samples (cTnI-WT and cTnI-ND) were scaled up or down relative to 100. Only modified phospho-peptides (Ser, Thr, Tyr) were considered for a roll-up of protein abundances and ratio calculation from grouped protein abundances. Hypothesis testing was performed using a *t* test based on the abundances of individual proteins or peptides with missing value imputation using low abundance resampling.

For analysis of the total, TMT reporter-based quantification was performed using a co-isolation threshold of 50, an average S/N threshold of 10, and an SPS mass match tolerance of 65%. Isotopic distribution corrections were applied to all channels based on Lot #TJ268160. Normalization, scaling, and calculation of total protein abundance ratios were similar to the phospho analysis above but using all peptides. Volcano plots were generated using protein or peptide isoform level data with *P*-value significance and fold-change cut-offs as indicated.

Statistical analysis

Western blots were analyzed with GraphPad Prism v 9.1.2. All comparisons were normally distributed (Shapiro–Wilk tested) and when equal variance (*F* test) an unpaired two-tailed *t* test was used; however, if the variance was unequal an unpaired two-tailed *t* test with Welch's correction was used for binary comparisons between cTnI-WT and cTnI-ND. The mean ± SEM was reported for all measurements with a *P*-value significance set at 0.05. Statistical analysis for the mass spectrometry data was done with Proteome Discoverer (version 2.3.0.523), which has integrated support for an unpaired two-tailed *t* test with Benjamini and Hochberg multiple testing correction. Significance was set at $P < 0.05$.

Bioinformatics analysis

The imported proteomic dataset from Proteome Discoverer included UniProt identifiers, phospho fold changes, and *P*-values, which were submitted to IPA for core analysis [12]. The core analysis was set to examine indirect and direct relationships between molecules based on observed

experimental phospho fold-change data in the IPA mouse database. The UniProt IDs were consolidated using the maximum measurement value in IPA. IPA was used to generate probable canonical pathways employing a right-tailed Fisher's exact test to calculate a *P*-value to explain the association between our dataset and the canonical pathway.

Results

Characterization of transgenic mice expressing N-terminal truncated cTnI in the heart

There are three muscle-type isoforms of troponin I in vertebrates: fast, slow, and cardiac versions (Fig. 1a). cTnI has a unique N-terminal extension that is an adult heart-specific structure. It has been previously shown [2] that there is an N-terminally truncated version of the cardiac troponin I that can be induced during conditions of stress by activating

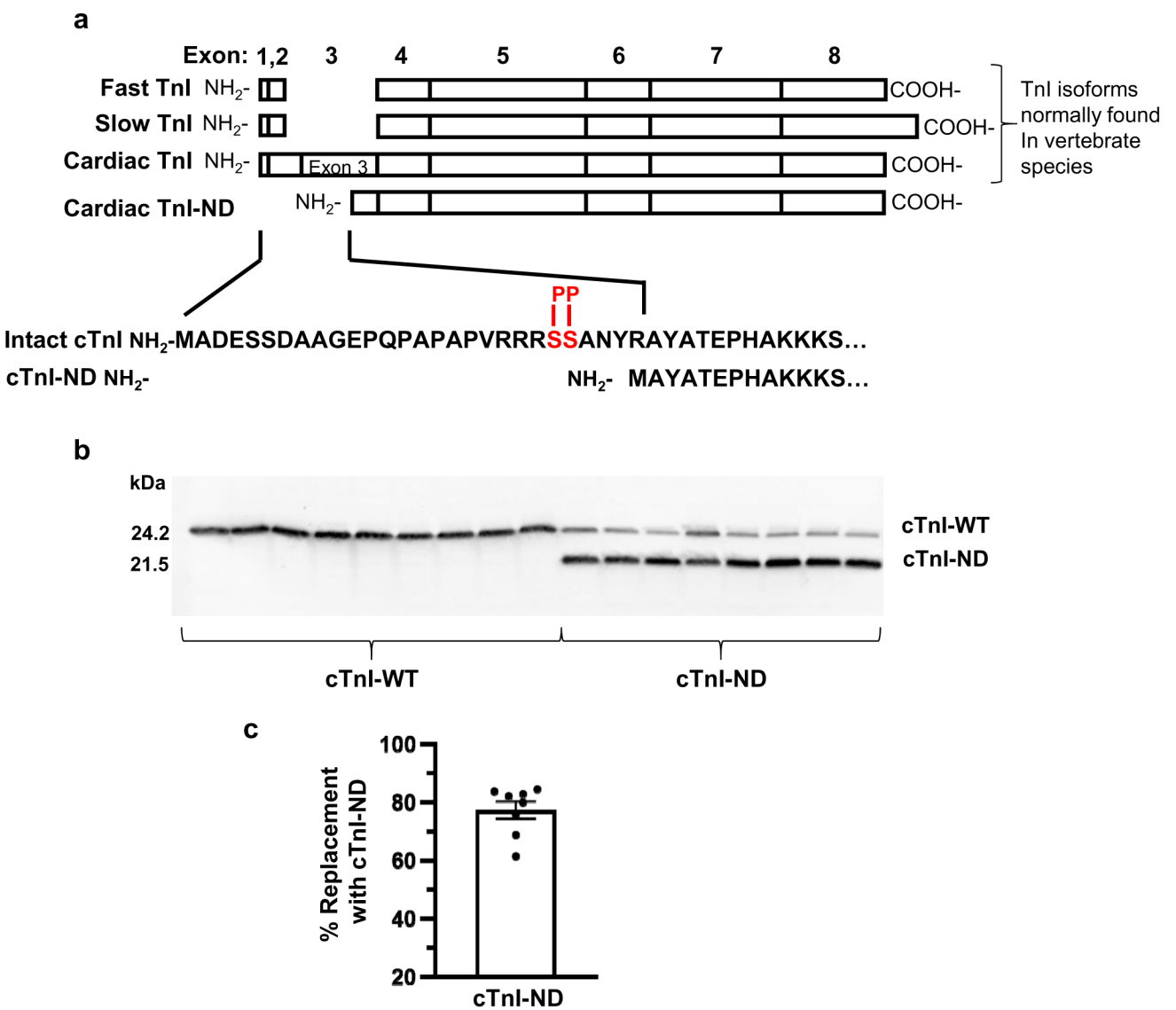

Fig. 1 Characterization of the transgenic cardiac troponin I (cTnI) N-terminal deleted (ND) mouse hearts. **a** Aligned structural maps of fast skeletal muscle troponin I (TnI) and slow skeletal muscle TnI, cTnI, and cTnI-ND indicating the location of the truncation relative to other isoforms of TnI. **b** Western blot probing the carboxyl end of cTnI. The non-transgenic littermates had no detectable cTnI-ND only the wildtype (WT). **c** Densitometry of the Western blot from **b** indicating the percent replacement with cTnI-ND in the transgenic animals. Data represented as mean ± SEM, $n = 8$

restrictive proteolysis (Fig. 1a). In the transgenic mouse line expressing the cTnI-ND, we determined the level of cTnI-ND replacement *vs* cTnI-WT which was ~ 77% in the myofilament fraction (Fig. 1b, c). The cTnI-WT animals did not have any detectable cTnI-ND (Fig. 1b). The overexpressing cTnI-ND transgenic mice were generated with the cloned promoter of the mouse cardiac α-myosin heavy chain gene to direct the specific expression of cTnI-ND (A.A. 29-211) to the cardiac myofilaments as previously described [7]. Previous findings from Barbado et al. [7] indicated that the removal of the N-terminal cTnI increased the relaxation rate and lowered the left ventricular end-diastolic pressure enhancing cardiac function.

cTnI-ND promotes compensatory effects beyond the myofilaments

To investigate the secondary adaptations from the direct effect of cTnI-ND on myofilament function and discover other mechanisms associated with the cardioprotective phenotype reported, we implemented a proteomic approach with an emphasis on global protein phosphorylation within the heart. Our workflow for digested whole heart samples (Fig. 2) utilized isobaric labeling for multiplexing and quantitation to assess phosphorylated peptides, total non-modified peptides, in conjunction with phospho-peptide enrichment via metal oxide affinity chromatography using both iron and titanium dioxide, and peptide fractionation to reduce sample complexity (Fig. 2). Using this approach, we identified 11,410 phospho-peptide isoforms (Fig. 3a, Supplementary Table S1), which yielded 1674 phosphorylated proteins from our proteomics workflow. The non-modified peptide isoforms (27,291) bore 2971 non-modified proteins (Fig. 3b, Supplementary Table S2). Only one protein (fumarylacetoacetase) exceeded the 1.5-fold-change cut-off; however, there were no phosphorylated peptides identified for this protein, thus it was excluded from our analysis (Fig. 3b, Supplementary Table S2). In addition, several housekeeping proteins (actin, tubulin, HDAC1, transferrin, vinculin) that showed similar abundance levels between cTnI-ND and cTnI-WT are bolded in the proteins tab of the Supplementary Table S2. Hence changes found in the phosphorylated peptides are likely due to signaling changes and not changes in total protein abundance between cTnI-ND and cTnI-WT or sample preparation differences. Based on our data, the predominant phenotypic effect associated with cTnI-ND expression in the myofilaments is not related to changes in protein abundance as often seen with the extensive remodeling in cardiomyopathies and other cardiac pathologies. This finding agrees with previously published studies showing this modification elicits an adaptive response, without impacting the morphology and geometry of the heart [7, 13]. Instead, cTnI-ND expression leads to post-translational alterations of the proteins within signaling pathways, without significant changes in their abundance.

As expected, some of the most significantly altered phospho-peptide isoforms were from cTnI and this served as an internal control for differences between cTnI-WT and cTnI-ND (Fig. 3a). There were 73 differentially phosphorylated proteins (31 decreased and 42 increased vs cTnI-WT) mapping to the identified peptides that were altered by at least a 1.5-fold change in cTnI-ND *vs* cTnI-WT (Supplementary Table S3). To gain insight into biological functions and potential signaling events associated with these 73 phospho-proteins, we analyzed our dataset using Ingenuity Pathway Analysis (IPA). IPA core analysis nominated the top 4 canonical pathways represented by our enriched phospho-protein pool, integrin, protein kinase A, RhoA, and actin cytoskeleton signaling pathways [$-\log(P\text{-value})$ 4.15 − 3.12] (Fig. 4a). A cropped portion of the top pathway, integrin, is shown with the color of the altered phosphorylated proteins identified within this pathway coded for changes in abundance (Fig. 4b). The integrin signaling pathway contains paxillin, an adapter protein found in the costameres of striated muscle in which phosphorylation was significantly reduced in the cTnI-ND group (Fig. 4b, Supplementary Table S3). In addition, Yap1 (Yes-Associated Protein 1) phosphorylation (S148 or S149) was significantly decreased in the cTnI-ND group (Supplementary Tables S1 and S3), which is a major protein component of the Hippo pathway involved in the control of cell proliferation, organ size, apoptosis, and cell fate.

Validation of paxillin and cTnI

Western blot analysis validated the mass spectrometry data in an orthogonal approach using antibodies. Phosphorylated cTnI abundance was determined with a specific antibody to S23/24 and was found to be very significantly reduced in the cTnI-ND vs. cTnI-WT, whereas the total abundance of cTnI (cTnI-WT + cTnI-ND) was not significantly altered based on a pan cTnI antibody (C-terminal epitope) staining both forms of cTnI (Fig. 5a). In the case of paxillin, we detected a significant decrease at Y31 in the cTnI-ND vs. cTnI-WT similar to what was found with mass spectrometry, even though it was not the exact site found in the mass spectrometry data (T249) (Fig. 5b, Supplementary Table S1). Unfortunately, commercially available site and phospho-specific paxillin antibodies to T249 were not available. However, we

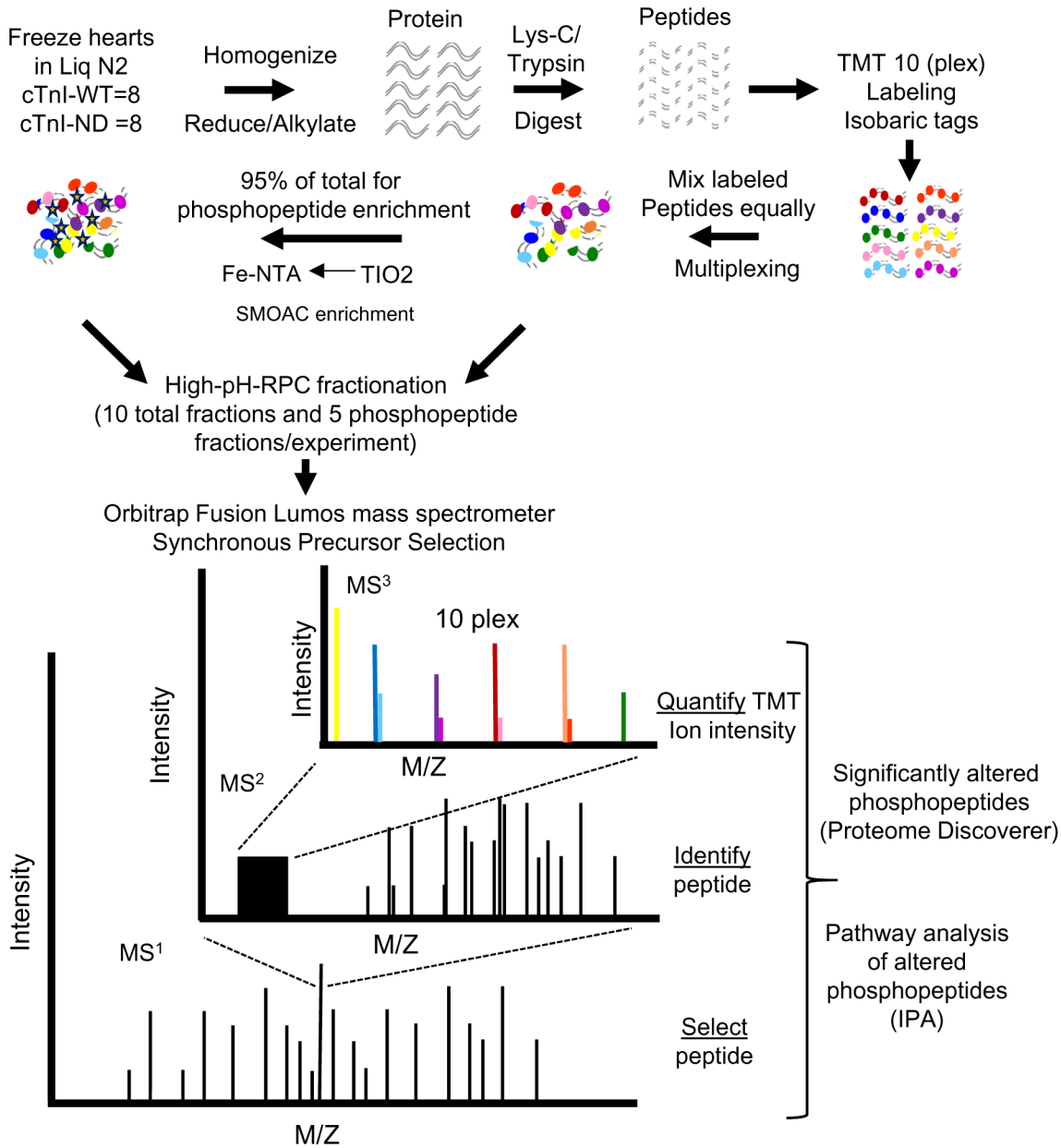

Fig. 2 Proteomic workflow used to compare wildtype (WT) vs transgenic cardiac troponin I (cTnI)-N-terminal truncated (cTnI-ND) mouse hearts. Stars depict phosphorylation and colored ovals indicate tandem mass tagged (TMT)-labeled peptides. Sequential enrichment of metal oxide affinity chromatography (SMOAC) facilitated the enrichment of phosphorylated peptides via titanium dioxide (TiO_2) and High-Select iron-nitrilotriacetate (Fe-NTA) affinity chromatography. High-pH reverse-phase chromatography (High-pH-RPC) fractionation was utilized to decrease sample complexity and increase peptide and protein identifications. Pathway and network analyses were performed with Ingenuity Pathway Analysis (IPA)

think both mass spectrometry and Western blot data indicate a likely reduction in paxillin phosphorylation in the cTnI-ND animal hearts. Collectively, our data indicate that the absence of the N-terminal 28 amino acids of cTnI-ND changes the intrinsic biophysical properties of the myofilaments to potentially signal protective mechano-sensing autocrine/paracrine signaling pathways or the myocyte's interactions with the extracellular environment.

Discussion

Our previous studies indicate that adaptive proteolytic cleavage of the N-terminal 28 amino acids of cTnI changes the intrinsic biophysical properties of the myofilaments, to correct aberrant events directly at the level of the contractile machinery. One novel finding here is that the

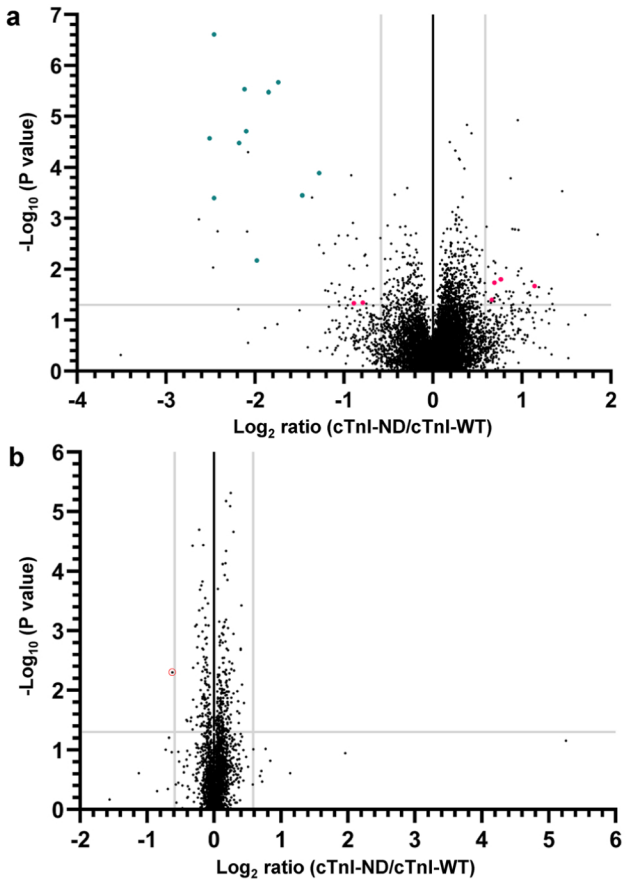

Fig. 3 Volcano plots indicating both peptide and protein distributions. **a** Phospho-peptide isoform distributions. Pink and teal-bolded spots indicate significantly altered phospho-peptides within the integrin pathway and cardiac troponin I, respectively. **b** Non-modified proteins with only one significantly altered protein (fumarylacetoacetase circled in red), which did not have a phospho-peptide identified and thus not included in the analysis. Vertical and horizontal gray lines indicate a 1.5-fold change in cTnI-ND vs cTnI-WT and $P < 0.05$ significance (via a two-tailed *t* test with Benjamini and Hochberg multiple testing correction) thresholds, respectively. Note as expected the cardiac troponin I had some of the most significantly altered phosphorylation levels as shown in **a** in teal

intrinsic signaling initiated by this modification in the myofilaments provokes adaptive signaling in the absence of remodeling of protein content and composition of the heart. Since the overall adaptive phenotype of cTnI-ND expression to pathological perturbation is documented [2, 3, 9, 13], defining these potential mechanisms and primary effects is not always best served within the context of the disease background. Consequently, our approach to investigate cTnI-ND vs cTnI-WT highlights some potentially important mechanistic post-translational events that might otherwise be lost in the complexity and amplification of signaling pathways in the disease state.

Functional and cardioprotective effects of cTnI-ND in relation to phospho-proteomic remodeling

Although there is strong evidence of altered signaling induced by the expression of cTnI-ND, our experiment provides the first comprehensive investigation of mechanisms. We set out to compare global phospho-proteomic profiles in the cardiac compartment of control mice and transgenic mice expressing cTnI-ND. Differences between the function of control and cTnI-ND hearts, which we have reported [1–3, 7, 9], are an important consideration in our interpretation of the phospho-proteomic profiling and pathway analysis reported here. These findings indicate the involvement of mechano-sensitive and kinase/phosphatase signaling pathways induced by the chronic presence of cTnI-ND in the heart, without changes in gross morphology or mass. Findings reported in our previous publications employing hearts of nearly the same age as those studied here showed no differences in heart weight/body weight ratios between controls and cTnI-ND hearts [7, 13]. These gross metrics correspond to the lack of change in the overall proteome abundance and composition between the control and cTnI-ND hearts (Fig. 3b, Supplementary Table S2) and underscores the significance of the changes in the post-translational profiles found in this study.

At 4 months of age, we have previously reported that compared to controls, skinned fibers isolated from transgenic (TG)-cTnI-ND mouse hearts show a decreased response to Ca^{2+}, a significant increase in steepness of the tension pCa relation, and an increase in tension cost as determined by simultaneous measurements of tension and ATP hydrolysis [9]. These data indicated that cross-bridge kinetics and thin filament deactivation are elevated with the presence of cTnI-ND. These changes occurred independently of a change in the population of α- and β-myosin heavy chain isoforms, again highlighting similar protein compositions. The analysis showed no phosphorylation at sites in the cTnI-ND and reduced phosphorylation in the remaining intact cTnI in the heart. In isolated working heart preparations, cTnI-ND hearts showed enhanced diastolic function [7]. Determination of in situ intra-ventricular pressures showed no change in $+dP/dt$, but a significant increase in $-dP/dt$ and decrease in LVEDP [7]. In studies employing echocardiographic assessment, we compared function in control hearts and cTnI-ND hearts in 16-month-old mice [9]. Compared to controls, cTnI-ND hearts in vivo demonstrated significant increases in fractional shortening, cardiac output, and velocity of circumferential shortening. Intraventricular relaxation time was significantly abbreviated in the cTnI-ND hearts compared to controls. Thus, the characteristics obtained from the isolated 4-month-old working hearts were sustained with aging indicating an adaptive response that does not decompensate over time. The functional effects

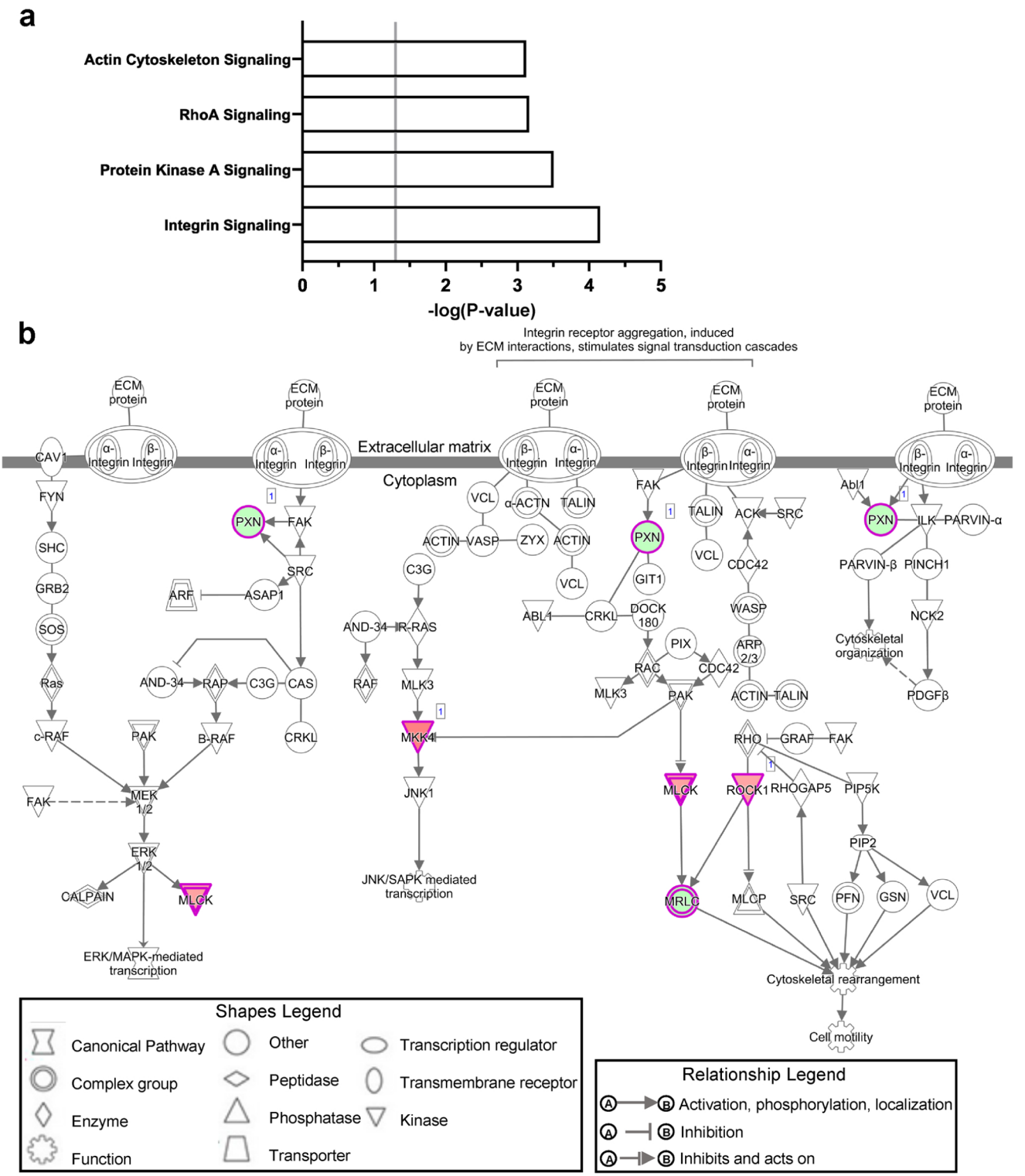

Fig. 4 Canonical pathways. **a** Bar chart of the 4 top canonical pathways, $P < 0.05$ (gray vertical demarcation line), generated by Ingenuity Pathway Analysis (IPA) (QIAGEN Inc.) software utilizing a right-tailed Fisher's exact test, based on significantly altered phosphorylation between wildtype and N-terminal deleted cardiac troponin I hearts. **b** Partially cropped Integrin pathway generated by IPA from significantly altered (cTnI-ND vs cTnI-WT) phosphorylated proteins shown in red (increased) or green (decreased). Solid line, direct interaction; slotted line, indirect interaction

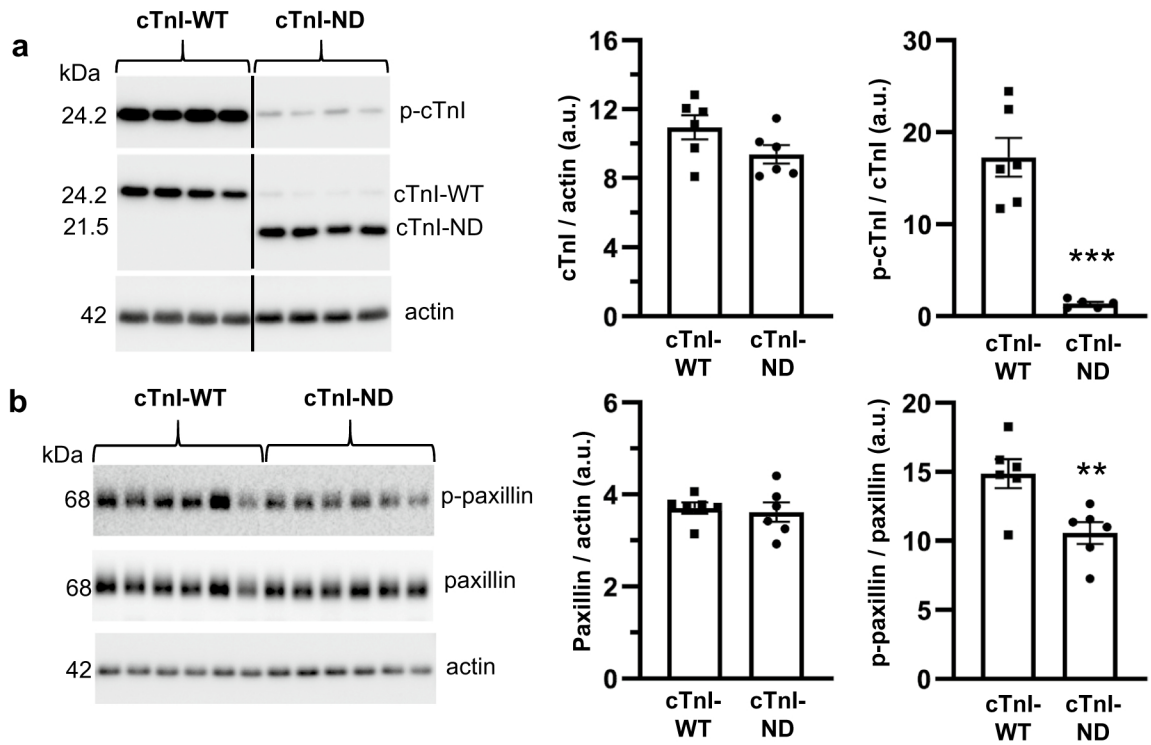

Fig. 5 Western blot validation of mass spectrometry data. N-terminal deleted cardiac troponin I (cTnI-ND) and wildtype cardiac troponin I were compared (cTnI-WT). **a** Representative Western blot images probed for phospho-cTnI S23/24, pan cTnI recognizing the C-terminus of cTnI, actin for loading control on the left side, and the quantitative histograms on the right indicating total (cTnI-WT + cTnI-ND) and phospho-abundance levels. Data were analyzed with an unpaired two-tailed *t* test with Welch's correction. **b** Western blot images probed for phospho-paxillin Y31, pan paxillin, actin for loading control on the left side, and the quantitative histograms on the right indicating total and phospho-abundance levels. Data were analyzed with an unpaired two-tailed *t* test. All data represented as mean ± SEM, $n = 5–6$, $^{**}P = 0.0079$, $^{***}P = 0.0003$

of expression of cTnI-ND, described above indicate likely modification of mechano-sensitive signals and post-translational modifications are cardioprotective in the context of aging [9], hemodynamic [2], and adrenergic stressors [3], rather than transcriptional and protein profile changes. Our hypothesis [4, 14–16] has been that sensing of the mechanical state of the sarcomeres occurs at the Z-disk in a network of two-way protein–protein interactions consisting of sarcomere force generating cross-bridges, thin filaments, and titin [17]. At the Z-disk, there are interactions via desmin to the stress-sensitive costamere-focal adhesion-integrin complex and extracellular matrix network. Results of our phospho-proteomic profiling support this reasoning.

Chronic presence of cTnI-ND induces mechano-signaling via the integrin cascade to downstream effectors and the Hippo pathway

Phosphorylation of peptides with ≥ 1.5-fold change as discovered in our proteomic analysis (Supplementary Table 3S; Fig. 3) comparing controls and TG-cTnI-ND hearts provide important information related to mechanisms of cardioprotection. Bioinformatic pathway analysis illustrated in Fig. 4 indicates that the persistent expression cTnI-ND is cardioprotective in part related to adaptive mechano-sensitive signaling pathways including the actin cytoskeleton, Rho A, PKA, and with a preponderance of integrin signaling. Integrins are heterodimeric transmembrane receptors transducing mechanical signals and consisting of α- and β-subunits with large extracellular domains making contact between the extracellular matrix and cardiac myocytes and fibroblasts [18, 19]. Linkage of the integrin, focal adhesion complex at the costamere to cytoskeletal networks modulates kinase/phosphatase signaling cascades as illustrated in Fig. 4 [14, 20]. An intracellular domain interacts with elements of the cytoskeleton including talin and kindlin [18, 19]. Talin and kindlin are involved in activating integrins and act to recruit mechano-transduction signaling proteins.

Induction of integrin signaling in response to mechanical stress occurs in cardiac myocytes and fibroblasts promoting fibrotic signaling [21]. We couch our initial discussion of the significance of the pathways in the analysis summarized in Fig. 4 on hypertrophic and fibrotic signaling. A finding related to fibrotic and hypertrophic signaling is the

significant downregulation of phosphorylation of paxillin. Reduced paxillin phosphorylation is a key element in integrin-related signaling cascades ultimately affecting downstream targets, which may be responsible for the protective effect of cTnI-ND expression.

This depression of paxillin phosphorylation may be indicative of the reduced activity of cSrc and focal adhesion kinase (FAK) tyrosine kinases in hearts expressing cTnI-ND. Src and FAK, together with paxillin, form a group of non-receptor tyrosine kinases, which transduce mechanical signals from the extracellular matrix via integrins [18, 20, 22]. There is ample evidence that pressure overload-induced hypertrophy and associated fibrosis are linked to activation of the integrin signaling with activation of FAK, cSrc, and paxillin [23–27]. Early studies by Ruwolf et al. [28] showed that cyclic stretch-induced activation of neonatal cardiac fibroblasts leads to an elevation of paxillin phosphorylation. Subsequent work indicated that pressure overload induced hypertrophic growth through activation of integrins to downstream cytoskeletal effectors [25]. It is reported that within minutes there is an activation of FAK followed by a time-dependent association of FAK with the cytoskeleton in a multi-component signaling complex [26] and other studies demonstrate elevated phosphorylation of cSrc, leading to downstream pathway activation in pressure overload [29]. The specificity of these effects has been recapitulated in vitro in cardiac myocytes treated with Arg-Gly-Asp (RGD peptide) to stimulate integrin signaling [23, 24]. However, more germane to the idea that aberrant sensing of the mechanical state of the sarcomeres by changes in the costamere-focal adhesion-integrin complex and extracellular matrix network sensing is the observation that paxillin phosphorylation by cSrc is increased by 25-fold in mouse hearts carrying the HCM R403Q-α-myosin heavy chain mutation which are known to exhibit diastolic dysfunction [30]. In this context, a plausible hypothesis suggests the suppression of paxillin phosphorylation in cTnI-ND hearts may relate to the enhanced state of myofilament relaxation during diastole in the hearts indicating a potential mechanism for protection against maladaptive stress signaling [7, 9]. In addition, the Src-paxillin association has also been linked to the YAP/TAZ signaling (Hippo pathway) in mammalian cells [31]. Our mass spectrometry data (Supplementary Table S3) indicate a significant decrease in the phosphorylation of YAP1 at either position S148 or S149 in cTnI-ND expressing hearts, which has been previously shown in hearts to be modulated in the context of the Hippo pathway [32]. The Hippo pathway is a major signaling pathway sensing the 3-D microenvironment of the cardiac myocyte, fibroblasts, and vascular compartment [33, 34]. Adverse activation of Hippo signaling has been reported to occur in the progression of pressure overload myocardial stress leading to diastolic dysfunction [35] like that of aging, which we have reported is improved in hearts expressing cTnI-ND [9]. Moreover, our bioinformatic analysis revealed that major elements of the Hippo signaling pathway are modified in cTnI-ND hearts. The Hippo signaling pathway elements have previously been shown to be associated with integrin [36], Rho A [35], PKA [37], and actin cytoskeletal signaling, which in our dataset were all altered in cTnI-ND vs cTnI-WT (Fig. 4). Therefore, it is plausible that the cTnI-ND modification turns off the Hippo pathway leading to YAP/TAZ nuclear localization and promotion of cell proliferation and survival [38]. These data demonstrate the significant effects of cTnI-ND in maintaining homeostasis by mechanisms beyond the myofilaments.

Conclusions and clinical implications

Discovery experiments reported here have revealed a mode of adaptive remodeling of myocardial signaling occurring due to modification of cTnI by restrictive NH_2-terminal truncation. Our results support the significance of the cTnI regulation that not only tunes cardiac muscle contractility but also serves as a mechanism to alter mechano-sensitive signaling pathways which can offset maladaptive responses to cardiac stressors. While the focus of this study was discovery in nature, future studies will be needed to further validate the findings of the study. Our data suggest that screening for compounds or small molecules targeting the cTnI-N terminus-cTnC interface or for promoting the adaptive restricted proteolysis of cTnI generating cTnI-ND may represent a valid therapeutic approach. Genetic-based studies aimed at preventing HCM disease progression in mice expressing the HCM mutant Tm-E180G by co-expression of the cTnI phospho-mimetic (cTnI-S23D, S24D), with desensitizing actions, like cTnI-ND, provides support for the therapeutic value of these approaches [39]. Furthermore, biochemical studies also demonstrate that exchange of endogenous cTnI with cTnI-ND in Tm-E180G myofilaments induces desensitization to Ca^{2+} [40]. Data presented here emphasize the potential that therapies relating to cTnI-ND will not only modify sarcomere response to Ca^{2+} but also promote adaptive signaling in mechano-biology cascades.

Supplementary Information The online version contains supplementary material available at https://doi.org/10.1007/s11010-022-04414-3.

Acknowledgements None.

Author contributions CMW contributed to writing of the original draft, writing, reviewing, & editing of the manuscript, methodology, investigation, validation, and formal analysis; MH contributed to investigation, formal analysis, and writing, reviewing, & editing of the manuscript; PHG contributed to writing of the original draft and writing, reviewing, & editing of the manuscript; HZF contributed to resources and writing, reviewing, & editing of the manuscript; AWH

contributed to resources, formal analysis, and writing, reviewing, & editing of the manuscript; BMW contributed to writing, reviewing, & editing of the manuscript; PPdT contributed to writing, reviewing, & editing of the manuscript and funding acquisition. JPJ conceptualized and contributed to funding acquisition and writing, reviewing, & editing of the manuscript; RJS contributed to writing of the original draft, writing, reviewing, & editing of the manuscript, conceptualization, and funding acquisition.

Funding This work was supported by NIH grants RO1 HL128468 (to BMW and RJS), PO1 HL062426 Project 1, 3, and Core C (to RJS, PPdT, CMW), and RO1 HL127691 (to JPJ, RJS, and PPdT). The content is solely the responsibility of the authors and does not necessarily represent the official views of the National Institutes of Health.

Data availability All data are contained within the article, supplementary data, or available from the corresponding author R. John Solaro, email: solarorj@uic.edu. The raw mass spectrometry data have been deposited in the ProteomeXchange Consortium (http://proteomecentral.proteomexchange.org) via the MassIVE partner repository (https://massive.ucsd.edu/ProteoSAFe/static/massive.jsp) with the dataset identifier MSV000087049.

Declarations

Conflict of interest R. John Solaro is a member of the Scientific Advisory Board of Cytokinetics, Inc., a consultant to Pfizer, Inc., and a member of the Heart Failure Advisory Board of Amgen. The authors declare no additional competing financial interests.

Ethical approval This article contains studies with animals and all animal protocols were approved by the animal care and use committee of the University of Illinois at Chicago, which also conforms to the "Guide for the Care and Use of Laboratory Animals" published by the United States National Institutes of Health, 8th edition, revised 2011.

References

1. Yu ZB, Bao JX, Ma J, Zhang LF, Jin JP (2000) Changes in myocardial contractility and contractile proteins after four weeks of simulated [correction of simulate] weightlessness in rats. J Gravit Physiol 7:147–148
2. Yu ZB, Zhang LF, Jin JP (2001) A proteolytic NH2-terminal truncation of cardiac troponin I that is up-regulated in simulated microgravity. J Biol Chem 276:15753–15760. https://doi.org/10.1074/jbc.M011048200
3. Feng HZ, Chen M, Weinstein LS, Jin JP (2008) Removal of the N-terminal extension of cardiac troponin I as a functional compensation for impaired myocardial beta-adrenergic signaling. J Biol Chem 283:33384–33393. https://doi.org/10.1074/jbc.M803302200
4. Solaro RJ, Henze M, Kobayashi T (2013) Integration of troponin I phosphorylation with cardiac regulatory networks. Circ Res 112:355–366. https://doi.org/10.1161/CIRCRESAHA.112.268672
5. Solaro RJ, Moir AJ, Perry SV (1976) Phosphorylation of troponin I and the inotropic effect of adrenaline in the perfused rabbit heart. Nature 262:615–617
6. Kachooei E, Cordina NM, Potluri PR, Guse JA, McCamey D, Brown LJ (2020) Phosphorylation of Troponin I finely controls the positioning of Troponin for the optimal regulation of cardiac muscle contraction. J Mol Cell Cardiol 150:44–53. https://doi.org/10.1016/j.yjmcc.2020.10.007
7. Barbato JC, Huang QQ, Hossain MM, Bond M, Jin JP (2005) Proteolytic N-terminal truncation of cardiac troponin I enhances ventricular diastolic function. J Biol Chem 280:6602–6609. https://doi.org/10.1074/jbc.M408525200
8. Salhi HE, Walton SD, Hassel NC, Brundage EA, de Tombe PP, Janssen PM, Davis JP, Biesiadecki BJ (2014) Cardiac troponin I tyrosine 26 phosphorylation decreases myofilament Ca2+ sensitivity and accelerates deactivation. J Mol Cell Cardiol 76:257–264. https://doi.org/10.1016/j.yjmcc.2014.09.013
9. Biesiadecki BJ, Tachampa K, Yuan C, Jin JP, de Tombe PP, Solaro RJ (2010) Removal of the cardiac troponin I N-terminal extension improves cardiac function in aged mice. J Biol Chem 285:19688–19698. https://doi.org/10.1074/jbc.M109.086892
10. Ryba DM, Warren CM, Karam CN, Davis RT 3rd, Chowdhury SAK, Alvarez MG, McCann M, Liew CW, Wieczorek DF, Varga P, Solaro RJ, Wolska BM (2019) Sphingosine-1-phosphate receptor modulator, FTY720, improves diastolic dysfunction and partially Reverses atrial remodeling in a Tm-E180G mouse model linked to hypertrophic cardiomyopathy. Circ Heart Fail 12:e005835. https://doi.org/10.1161/CIRCHEARTFAILURE.118.005835
11. Erickson BK, Jedrychowski MP, McAlister GC, Everley RA, Kunz R, Gygi SP (2015) Evaluating multiplexed quantitative phosphopeptide analysis on a hybrid quadrupole mass filter/linear ion trap/orbitrap mass spectrometer. Anal Chem 87:1241–1249. https://doi.org/10.1021/ac503934f
12. Kramer A, Green J, Pollard J Jr, Tugendreich S (2014) Causal analysis approaches in ingenuity pathway analysis. Bioinformatics 30:523–530. https://doi.org/10.1093/bioinformatics/btt703
13. Li Y, Charles PY, Nan C, Pinto JR, Wang Y, Liang J, Wu G, Tian J, Feng HZ, Potter JD, Jin JP, Huang X (2010) Correcting diastolic dysfunction by Ca2+ desensitizing troponin in a transgenic mouse model of restrictive cardiomyopathy. J Mol Cell Cardiol 49:402–411. https://doi.org/10.1016/j.yjmcc.2010.04.017
14. Solaro CR, Solaro RJ (2020) Implications of the complex biology and micro-environment of cardiac sarcomeres in the use of high affinity troponin antibodies as serum biomarkers for cardiac disorders. J Mol Cell Cardiol 143:145–158
15. Pyle WG, Solaro RJ (2004) At the crossroads of myocardial signaling: the role of Z-discs in intracellular signaling and cardiac function. Circ Res 94:296–305. https://doi.org/10.1161/01.Res.0000116143.74830.A9
16. Solaro RJ (2005) Remote control of A-band cardiac thin filaments by the I-Z-I protein network of cardiac sarcomeres. Trends Cardiovasc Med 15:148–152. https://doi.org/10.1016/j.tcm.2005.04.007
17. Solis C, Solaro RJ (2021) Novel insights into sarcomere regulatory systems control of cardiac thin filament activation. J Gen Physiol. https://doi.org/10.1085/jpg.202012777
18. Parker KK, Ingber DE (2007) Extracellular matrix, mechanotransduction and structural hierarchies in heart tissue engineering. Philos Trans R Soc Lond B 362:1267–1279. https://doi.org/10.1098/rstb.2007.2114
19. Chen C, Li R, Ross RS, Manso AM (2016) Integrins and integrin-related proteins in cardiac fibrosis. J Mol Cell Cardiol 93:162–174. https://doi.org/10.1016/j.yjmcc.2015.11.010
20. Sit B, Gutmann D, Iskratsch T (2019) Costameres, dense plaques and podosomes: the cell matrix adhesions in cardiovascular mechanosensing. J Muscle Res Cell Motil 40:197–209. https://doi.org/10.1007/s10974-019-09529-7
21. Manso AM, Kang SM, Ross RS (2009) Integrins, focal adhesions, and cardiac fibroblasts. J Investig Med 57:856–860. https://doi.org/10.2310/JIM.0b013e3181c5e61f
22. Samarel AM (2014) Focal adhesion signaling in heart failure. Pflugers Arch 466:1101–1111. https://doi.org/10.1007/s00424-014-1456-8

23. Willey CD, Balasubramanian S, Rodriguez Rosas MC, Ross RS, Kuppuswamy D (2003) Focal complex formation in adult cardiomyocytes is accompanied by the activation of beta3 integrin and c-Src. J Mol Cell Cardiol 35:671–683. https://doi.org/10.1016/s0022-2828(03)00112-3
24. Laser M, Willey CD, Jiang W, Gt C, Menick DR, Zile MR, Kuppuswamy D (2000) Integrin activation and focal complex formation in cardiac hypertrophy. J Biol Chem 275:35624–35630. https://doi.org/10.1074/jbc.M006124200
25. Kuppuswamy D, Kerr C, Narishige T, Kasi VS, Menick DR, Gt C (1997) Association of tyrosine-phosphorylated c-Src with the cytoskeleton of hypertrophying myocardium. J Biol Chem 272:4500–4508. https://doi.org/10.1074/jbc.272.7.4500
26. Franchini KG, Torsoni AS, Soares PH, Saad MJ (2000) Early activation of the multicomponent signaling complex associated with focal adhesion kinase induced by pressure overload in the rat heart. Circ Res 87:558–565. https://doi.org/10.1161/01.res.87.7.558
27. Frangogiannis NG (2019) Cardiac fibrosis: cell biological mechanisms, molecular pathways and therapeutic opportunities. Mol Aspects Med 65:70–99. https://doi.org/10.1016/j.mam.2018.07.001
28. Ruwhof C, Egas JM, van Wamel AE, van der Laarse A (2001) Signal transduction of mechanical stress in myocytes and fibroblasts derived from neonatal rat ventricles. Netherlands Heart J 9:372–378
29. Wang S, Gong H, Jiang G, Ye Y, Wu J, You J, Zhang G, Sun A, Komuro I, Ge J, Zou Y (2014) Src is required for mechanical stretch-induced cardiomyocyte hypertrophy through angiotensin II type 1 receptor-dependent β-arrestin2 pathways. PLoS ONE 9:e92926. https://doi.org/10.1371/journal.pone.0092926
30. Xu M, Bermea KC, Ayati M, Yang X, Fu Z, AmirHeravi, Zhang X, Na C, Everett A, Gabrielson K, Foster DB, Paolocci N, Murphy AM and Ramirez-Correa GA (2020) Altered tyrosine phosphorylation of cardiac proteins prompts contractile dysfunction in hypertrophic cardiomyopathy. Research Square
31. Wang S, Englund E, Kjellman P, Li Z, Ahnlide JK, Rodriguez-Cupello C, Saggioro M, Kanzaki R, Pietras K, Lindgren D, Axelson H, Prinz CN, Swaminathan V, Madsen CD (2021) CCM3 is a gatekeeper in focal adhesions regulating mechanotransduction and YAP/TAZ signalling. Nat Cell Biol 23:758–770. https://doi.org/10.1038/s41556-021-00702-0
32. Aharonov A, Shakked A, Umansky KB, Savidor A, Genzelinakh A, Kain D, Lendengolts D, Revach OY, Morikawa Y, Dong J, Levin Y, Geiger B, Martin JF, Tzahor E (2020) ERBB2 drives YAP activation and EMT-like processes during cardiac regeneration. Nat Cell Biol 22:1346–1356. https://doi.org/10.1038/s41556-020-00588-4
33. Dasgupta I, McCollum D (2019) Control of cellular responses to mechanical cues through YAP/TAZ regulation. J Biol Chem 294:17693–17706. https://doi.org/10.1074/jbc.REV119.007963
34. Ma S, Meng Z, Chen R, Guan KL (2019) The hippo pathway: biology and pathophysiology. Annu Rev Biochem 88:577–604. https://doi.org/10.1146/annurev-biochem-013118-111829
35. Byun J, Del Re DP, Zhai P, Ikeda S, Shirakabe A, Mizushima W, Miyamoto S, Brown JH, Sadoshima J (2019) Yes-associated protein (YAP) mediates adaptive cardiac hypertrophy in response to pressure overload. J Biol Chem 294:3603–3617. https://doi.org/10.1074/jbc.RA118.006123
36. Yamashiro Y, Thang BQ, Ramirez K, Shin SJ, Kohata T, Ohata S, Nguyen TAV, Ohtsuki S, Nagayama K, Yanagisawa H (2020) Matrix mechanotransduction mediated by thrombospondin-1/integrin/YAP in the vascular remodeling. Proc Natl Acad Sci USA 117:9896–9905. https://doi.org/10.1073/pnas.1919702117
37. Yu FX, Zhang Y, Park HW, Jewell JL, Chen Q, Deng Y, Pan D, Taylor SS, Lai ZC, Guan KL (2013) Protein kinase A activates the Hippo pathway to modulate cell proliferation and differentiation. Genes Dev 27:1223–1232. https://doi.org/10.1101/gad.219402.113
38. Boopathy GTK, Hong W (2019) Role of hippo pathway-YAP/TAZ signaling in angiogenesis. Front Cell Dev Biol 7:49. https://doi.org/10.3389/fcell.2019.00049
39. Alves ML, Dias FA, Gaffin RD, Simon JN, Montminy EM, Biesiadecki BJ, Hinken AC, Warren CM, Utter MS, Davis RT 3rd, Sadayappan S, Robbins J, Wieczorek DF, Solaro RJ, Wolska BM (2014) Desensitization of myofilaments to Ca2+ as a therapeutic target for hypertrophic cardiomyopathy with mutations in thin filament proteins. Circ Cardiovasc Genet 7:132–143. https://doi.org/10.1161/CIRCGENETICS.113.000324
40. Warren CM, Halas M, Feng HZ, Wolska BM, Jin JP, Solaro RJ (2021) NH2-terminal cleavage of cardiac troponin I signals adaptive response to cardiac stressors. J Cell Signal 2:162–171